

Fundamentals of Refractory Technology

Edited by
James P. Bennett
Jeffery D. Smith

Ceramic
Transactions
Volume 125

Fundamentals of Refractory Technology

Related titles published by The American Ceramic Society:

Boing-Boing the Bionic Cat and the Jewel Thief

By Larry L. Hench

©2001, ISBN 1-57498-129-3

Boing-Boing the Bionic Cat

By Larry L. Hench

©2000, ISBN 1-57498-109-9

The Magic of Ceramics

By David W. Richerson

©2000, ISBN 1-57498-050-5

Ceramic Innovations in the 20th Century

Edited by John B. Wachtman Jr.

©1999, ISBN 1-57498-093-9

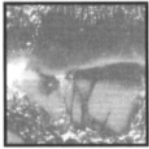
Monolithic Refractories

By Subrata Banerjee

©1997, ISBN 981-02-3120-2

For information on ordering titles published by The American Ceramic Society, or to request a publications catalog, please contact our Customer Service Department at 614-794-5890 (phone), 614-794-5892 (fax), <customersrvc@acers.org> (e-mail), or write to Customer Service Department, 735 Ceramic Place, Westerville, OH 43081, USA.

Visit our on-line book catalog at <www.ceramics.org>.



**Ceramic
Transactions**
Volume 125

Fundamentals of Refractory Technology

Proceedings of the Refractory Ceramics Division Focused Lecture Series presented at the 101st and 102nd Annual Meetings held April 25–28, 1999, in Indianapolis, Indiana, and April 30–May 3, 2000, in St. Louis, Missouri, respectively.

Edited by

James P. Bennett

U.S. Department of Energy
Albany Research Center

Jeffery D. Smith

University of Missouri—Rolla

Published by

The American Ceramic Society
735 Ceramic Place
Westerville, Ohio 43081
www.ceramics.org

Proceedings of the Refractory Ceramics Division Focused Lecture Series presented at the 101st and 102nd Annual Meetings held April 25–28, 1999, in Indianapolis, Indiana, and April 30–May 3, 2000, in St. Louis, Missouri, respectively.

Copyright 2001, The American Ceramic Society. All rights reserved.

Statements of fact and opinion are the responsibility of the authors alone and do not imply an opinion on the part of the officers, staff, or members of The American Ceramic Society. The American Ceramic Society assumes no responsibility for the statements and opinions advanced by the contributors to its publications or by the speakers at its programs. Registered names and trademarks, etc., used in this publication, even without specific indication thereof, are not to be considered unprotected by the law.

No part of this book may be reproduced, stored in a retrieval system, or transmitted in any form or by any means, electronic, mechanical, photocopying, microfilming, recording, or otherwise, without written permission from the publisher.

Authorization to photocopy for internal or personal use beyond the limits of Sections 107 and 108 of the U.S. Copyright Law is granted by the American Ceramic Society, provided that the appropriate fee is paid directly to the Copyright Clearance Center, Inc., 222 Rosewood Drive, Danvers, MA 01923 USA, www.copyright.com. Prior to photocopying items for educational classroom use, please contact Copyright Clearance Center, Inc.

This consent does not extend to copying items for general distribution or for advertising or promotional purposes or to republishing items in whole or in part in any work in any format.

Please direct republication or special copying permission requests to Copyright Clearance Center, Inc., 222 Rosewood Drive, Danvers, MA 01923 USA 978-750-8400; www.copyright.com.

Cover photo: "Dense MgO layer formed in the used MgO-C refractory with Al-Mg alloy," is courtesy of A. Yamaguchi, and appears as figure 10 in the paper "Application of Thermochemistry to Refractories," which begins on page 157.

Library of Congress Cataloging-in-Publication Data

A CIP record for this book is available from the Library of Congress.

For information on ordering titles published by The American Ceramic Society, or to request a publications catalog, please call 614-794-5890.

Printed in the United States of America.

4 3 2 1-04 03 02 01

ISSN 1042-1122

ISBN 1-57498-133-1



Contents

Preface vii

1999 Focused Sessions—Indianapolis, Indiana, April 26, 1999

**Particle Size Distribution as a Predictor of
Suspension Flow Behavior 3**

R.M. German

Rheology and Plasticity for Ceramic Processing 29

W.M. Carty

**The Nature of Chemical Reactions That Occur
During Castable Installation and Analytical Techniques
Used to Follow These Reactions 53**

C.D. Parr, C. Revais, and H. Fryda

**High-Temperature Mechanical Behavior of
Magnesia–Graphite Refractories. 73**

C. Baudin

**Needed Fundamental Thermomechanical Material
Properties for Thermomechanical Finite Element
Analysis of Refractory Structures. 93**

C.A. Schacht

**Porous Ceramic Simulation of Reservoir Rocks
Determination of Porosity by Electric
Permittivity Measurements. 103**

J. Lira-Olivares, D. Marcano, C. Lavelle, and F. Sánchez

Corrosion of Industrial Refractories. 135

M. Rigaud

2000 Focused Sessions—St. Louis, Missouri, May 1, 2000

| | |
|---|------------|
| Application of Thermochemistry to Refractories | 157 |
| A. Yamaguchi | |
| Creep Measurement and Analysis of Refractories. | 171 |
| J.G. Hemrick and A.A. Wereszczak | |
| Corrosion of Refractories in Glass-Melting Application | 195 |
| S.M. Winder and K.R. Selkregg | |
| Oxyfuel Firing Effects on Refractories | 223 |
| R.E. Moore, M. Velez, M. Karakus, and W.D. Headrick | |
| Cold Setting Cordierite Castables | 235 |
| E.F. Aglietti, N.E. Hipedinger, and A.N. Scian | |
| Different Types of <i>in situ</i> Refractories | 245 |
| W.E. Lee, S. Zhang, and H. Sarpoolaky | |
| The Use of Modeling in Refractories | 253 |
| C.E. Semler | |
| Bath Penetration of Barrier Refractories for Aluminum Electrolytic Cells | 261 |
| G. Oprea | |
| Interfacial Phenomena | 289 |
| C. Allaire | |
| Index | 309 |



Preface

This volume contains papers presented in focussed sessions of two Refractory Ceramics Division (RCD) meetings held in conjunction with the 101st Annual Meetings & Expositions (Indianapolis, Indiana—April 25–28, 1999) and the 102nd Annual Meeting and Exposition (St. Louis, Missouri—April 30–May 3, 2000). The focussed sessions were organized by RCD and the editors of this volume. Refractory scientists from throughout the world were invited to provide overviews of the scientific principles related to refractory manufacturing and performance. The sessions were well received, with at times as many as 100 scientists and engineers from industry, university, and government laboratories in attendance.

This book contains seven of eight papers presented during the 1999 Focused Sessions and nine of the 11 papers presented during the 2000 Focused Sessions. One paper for the 2000 Focused Session ("A Novel Rhoemeter for Refractory Castables," by Pandolfelli, Pileggi, and Paiva) was published in the *American Ceramic Society Bulletin*. The papers were reviewed by committee. The editors would like to recognize the balance of the committee and thank them for their assistance. They include Dr. Richard C. Bradt, University of Alabama, Dr. Robert E. Moore, University of Missouri—Rolla, and Dr. Michel A. Rigaud, École Polytechnique.

The editors are especially grateful for the efforts of the authors who presented in the focused sessions and were diligent in completing their manuscripts. In addition, the editors would like to thank all those individuals who attended the technical sessions. It is our hope that the information presented in the focused sessions and contained in this book will help advance knowledge in refractory science.

Jeffery D. Smith
James P. Bennett

1999 Focused Sessions

Indianapolis, IN, April 26, 1999

Dr. Jeffery D. Smith, Program Chair
Department of Ceramic Engineering
University of Missouri - Rolla
Rolla, MO, USA

Dr. Michel A. Rigaud, Session Chair
École Polytechnique
Montreal, Canada

Dr. Richard C. Bradt, Session Chair
University of Alabama
Tuscaloosa, AL, USA

PARTICLE SIZE DISTRIBUTION AS A PREDICTOR OF SUSPENSION FLOW BEHAVIOR

Randall M. German
Brush Chair Professor in Materials
Center for Innovative Sintered Products
P/M Lab, 147 Research West
The Pennsylvania State University
University Park, PA 16802-6809, USA

ABSTRACT

Component fabrication from powder suspensions has many variants and they all have magic particle size distributions that give improved behavior. Distributions that give the highest packing density and lowest forming viscosity have been known for decades. Size distributions with high packing densities and low flow viscosities characteristically are wide with an abundance of large particles. This presentation shows examples from several powder mixtures to illustrate links between particle packing and mixture viscosity. Operative principles and distribution parameters provide insight on suspension viscosity and yield strength. Homogeneity is the largest source of error between theory and practice, so principles are introduced for measuring homogeneity.

INTRODUCTION

An understanding of particle packing characteristics is important in many common ceramic forming operations, ranging from slip casting to reaction bonding. Most important, an understanding of packing density is an invaluable basis for understanding rheology in powder processing. The study of particle packing is well documented in three books [1-3]. Packing density describes the volume fraction of a container that is filled with powder and is measured by fractional density. The rheology of a powder suspension is measured by the stress needed to initiate flow and the resistance to sustained flow as measured by the viscosity. The goal is to induce a high packing density via mixed particle sizes or continuous particle size distributions, recognizing this results in low viscosity

To the extent authorized under the laws of the United States of America, all copyright interests in this publication are the property of The American Ceramic Society. Any duplication, reproduction, or republication of this publication or any part thereof, without the express written consent of The American Ceramic Society or fee paid to the Copyright Clearance Center, is prohibited.

suspensions.

Many industrial situations have proprietary links between the particle size, particle shape, distribution width, packing density, and processing. Detailed relations are beyond the scope of this article; however, it is important to recognize that packing density is an easily measured attribute that provides much insight into powder flow [4], viscosity [5], elasticity [6], compaction [7], infiltration [8], sintering [9], permeation [10], molding [11], melting [12], hot isostatic compaction [13], and other attributes. Indeed, the problem of optimizing particle size distributions to improve packing density and flow is encountered in many fields, including chocolate, ice cream, filled polymer molding, asphalt, cement, solder pastes, paints, slip casting, thixomolding, powder metallurgy, tape casting, and castable refractories.

Although refractory systems are the focus of the seminar series, major interest arises from studies on the flow behavior of powders used in powder injection molding [14]. A powder and thermoplastic polymer mixture are mixed to form a viscous slurry that can be molded into a cold die cavity. The polymer freezes in the die to hold the particles in the cavity shape. The particle size distribution and particle shape determine the solids loading (ratio of powder volume to total volume) in the feedstock, which controls the viscosity and subsequent processing steps. The lower the packing density of the powder, the greater the binder content needed for flow. Generally, in selecting a powder for a process, the desire is to attain a high solids loading, recognizing that such powders require less polymer for molding and sintering shrinkage for densification.

Packing structures are categorized as either random or ordered. As shown in Figure 1, a random packing is constructed by a sequence of events that are not correlated with one another. When a powder is poured into a container, the structure is random. On the other hand, an ordered structure occurs when objects are placed systematically into periodic positions, such as the stacking of bricks to form a wall. Random structures lack long-range repetition, and typically exhibit lower packing densities.

For monosized spheres the maximum packing density occurs in an ordered close-packed array with a coordination number of 12 and a density of 74%. With respect to most ceramic powders, the highest packing density is random and the structure forms with a density less than that for ideal, monosized spheres at 60 to 64%. Tap density, the highest density random packing, occurs when the particles have been vibrated without introducing long range order or deformation. The random loose packing that results when particles are poured into a container without agitation or vibration is commonly called the apparent density.

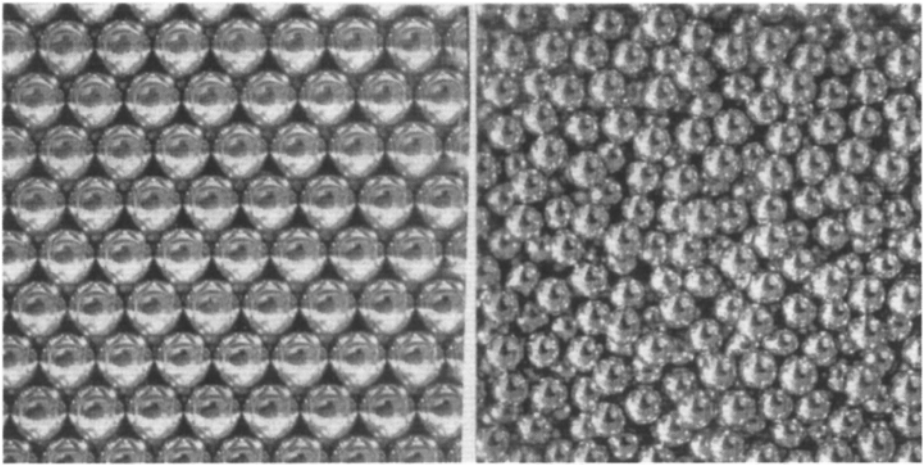


Figure 1. Pictures contrasting the structure for a random and ordered array of monosized spheres.

fractional density

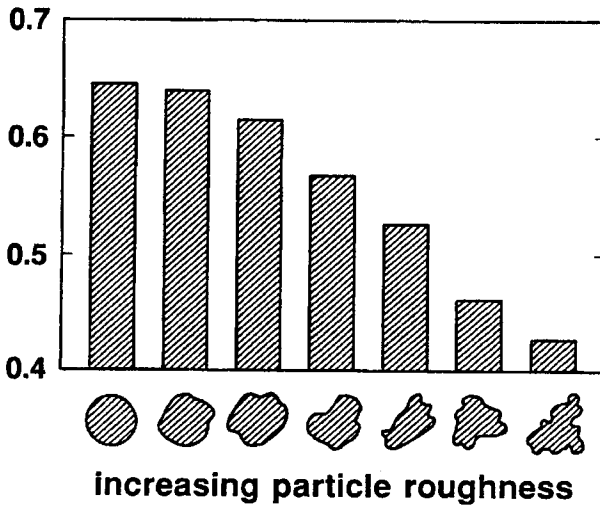


Figure 2. Packing density for random monosized particles as a function of the particle shape and surface roughness, showing the benefit of equiaxed and smooth particles.

HISTORICAL INTEREST IN PACKING AND SUSPENSION FLOW

Concern over particle packing and flow traces back at least 300 years. A detailed history on particle packing is available in reference [1-3] and the implications with respect to rheology are covered in references [14-19]. Today we recognize that a coordination number of 12 is the highest possible for monosized spheres (the close-packed structure evident in crystallography). However, Newton in 1694 speculated on the creation of a high packing density structure with 13-fold coordination. Hales in 1727 examine the packing of peas, using dried peas that swelled in water to form flat contact faces, allowing first determination of the relation between packing density and coordination number. Einstein treated the problem of dilute suspension flow in 1906, proposing a linear relation between viscosity and solids loading. About this same time, Fuller and Thompson in 1907 were constructing earthen dams for the New York City water system and explored relations between rock-gravel-sand grain size distribution and the mixture density and strength. Their findings are valuable today, showing four rules for creation of high strength dams (which happen to be those with high packing densities):

- use the largest mean particle size possible
- use rounded particles
- skew the size distribution to use a high fraction of large particles
- rely on a low volume of intermediate sized particles.

Subsequent studies showed these concepts were very accurate and extended to continuous particle size distributions. Important conceptualizations were provided by Furnas in 1928 and Andreasen in 1930, both suggesting that optimal distributions could be envisioned based on filling space first with the largest particles. Subsequently, smaller particles are selected to fill the voids, and at each subsequent level smaller particles are used to fill remaining void space. From a demonstration view, McGeary in 1961 showed a five-mode particle mixture with a packing density of 95%. About this same time, Scott experimentally determined the maximum packing density obtainable with monosized spheres. Meanwhile, interest in viscosity was related to the maximum packing density, and the work of Money in 1950 proved most accurate in showing that viscosity of a suspension is directly linked to the maximum packing density.

It is on this base that today we look at the effect of particle size distribution on packing as a precursor problem to a study of suspension rheology. Fundamentally, high packing density powders also have low suspension viscosities for a given powder content.

KEY FACTORS

The particle characteristics important to ceramic processing are packing density, strength, surface area, permeability, and pore size. A critical characteristic is packing density. For example, in powder injection molding, the required quantity of binder approximately equals the void space between particles [20]. Optimal quantities of binder ensure defect-free molding. Likewise, many other processing factors, including sintering shrinkage, debinding rate, and compact strength depend on the packing density.

Particles of differing materials, but equal size and shape, will pack to the same fractional density in spite of differing theoretical densities. However, several other factors cause differences in packing densities. For a mean particle size below approximately 100 μm there is more interparticle friction to inhibit packing; thus, for small particles the loose random packing density is a function of the mean particle diameter [3,21]. Part of the problem arises because of agglomeration, since surface forces are large when compared to the particle mass. This problem is most apparent as the particle size decreases below approximately 1 μm . One option is to create repulsive forces between particles by using thin surface coatings of polar molecules or control of the powder surface charge via pH adjustment. The surface repulsive forces contribute to high packing densities by reducing the interparticle friction. Thus, attention to surface chemistry is beneficial in formulating powder mixtures requiring high packing densities.

Another form of interparticle friction arises from surface irregularities on the particles. The greater the surface roughness or the more irregular the particle shape, the lower the packing density. Data for the particle shape effect on packing density are scattered, yet some general patterns are apparent. A higher packing density is associated with spherical particles with smooth surfaces. For particles of the same size but different shapes, the packing density will decrease as the shape departs from spherical or equiaxed [3,22].

When two or more powders are mixed together, there will be opportunities to improve the packing density. However, this assumes the structure is homogeneous, with the small particles ideally situated in the voids between the large particles. Although the ideal is simple to describe, there is still difficulty in attaining the desired homogeneity. The best symptom of inhomogeneity is the viscosity and instability of the viscosity [23]. A related problem with wide particle size distributions is segregation based on particle size. Size segregation is more of a problem with large mean particle sizes and large differences in particle size. One consequence of size segregation is a decrease in the overall mixture density and point-to-point density variations. In well-mixed powders, size segregation is not a serious problem. Organic processing aids are used to minimize segregation in handling, especially for smaller powders that exhibit

poor flow and packing.

For highest densities, it is appropriate to vibrate the powder to eliminate bridging, large voids, or other defects. For this reason, the tap density provides a best first measure of particle packing and proves relevant to many forming operations. The measurement depends on the material, vibration amplitude, vibration direction, applied pressure, vibration frequency, particle density, shear, and test apparatus [24,25]. During vibration the density varies with the number of vibrations by an exponential function,

$$f(N) = f_i + (f_f - f_i) \exp\left(-\frac{K}{N}\right) \quad (1)$$

where K is a constant that depends on the device, height of fall, and velocity, N is the number of vibration cycles, f_f is the final solids density, $f(N)$ is the solids density after N cycles, and f_i is the initial solids density. Generally, the more irregular the particle shape, the greater the packing benefit from vibration. Powders will reach the dense random packing limit more rapidly as the particle size increases.

IDEAL PACKING

As a starting point, consider the packing of an ideal powder, where each particle is the same size and spherical. This is probably the best studied packing problem, yet it is far from the typical powders. It is the basis for most models, partly because of similarities to hard sphere models for crystalline atomic structure - body-centered cubic, face-centered cubic, and simple cubic packings.

An ordered packing consists of perfectly placed spheres. Many common examples are known in crystallography tables; for example the body-centered cubic structure is 68% dense. There is a systematic increase in packing density as the number of contacts per sphere increases. The highest packing for monosized spheres is a coordination number of 12 with a 74% density. On the other hand, the lowest possible packing density in a gravitationally stable structure formed from nonadhesive spheres is a coordination number of 4 with a packing density near 34%.

Various models link the coordination number and packing density. Unfortunately there is no exact relation between packing density and coordination number, but a simple model is,

$$N_c = 2 \exp(2.4 f) \quad (2)$$

where N_C is the packing coordination number and f is the fractional density.

An important packing with respect to ceramic processing is the random dense structure. This is formed by vibrating a powder into a high packing density without the application of external stress, other than gravity. For the monosized spheres, this packing density is 63.7% [26], which equals $2/\pi$. As a point of comparison, the packing density of a random loose array of monosized spheres is 60%, with approximately 6 contacts per sphere. Such a structure forms when uniform spheres are poured into a container, but not vibrated.

The random dense packing and random loose packing are fairly similar for large spherical particles. Consequently, spherical particles of sizes greater than approximately 100 μm undergo little densification during vibration. In contrast, smaller spheres and nonspherical particles exhibit a greater difference between the apparent and tap densities. These particles undergo a larger packing density increase with vibration and exhibit higher packing densities in the presence of fluids, surfactants, and pressure.

The packing density and coordination number decrease as the particle shape departs from that of a sphere. Figure 2 shows the fractional packing density for various monosized irregular particle shapes. Powders with highly irregular particle shapes do not match the packing density for spheres. As the particle shape becomes more rounded (spherical) the packing density increases. The difference between random and ordered packing densities increases as the particle shape becomes nonspherical.

Spherical or rounded particles are desirable in applications that require a high packing density and easy flow. But if the particle has a regular polygonal shape, then a decrement in packing density does not always occur. Anisotropic particles can be packed to high densities if they are ordered. For example, cubic particles can be packed to 100% density when placed in an ordered packing. The highest packing densities and most isotropic structures are observed with equiaxed particles, such as spheres and cubes. Fibers in random packing exhibit a decrease in density as the length-to-diameter ratio increases [27]. Fractional densities below 10% result from random packing of fibers with large length-to-diameter ratios.

BIMODAL MIXTURES OF SPHERES

Basic Structure - Bimodal particle mixtures pack to higher densities than do monosized particles. The key to improved packing rests with the particle size ratio. Small particles are selected such that they fit into the interstices between large particles without forcing the large particles apart. In turn, even smaller particles can be selected to fit into the remaining pores, giving a corresponding improvement in packing density.

To improve the packing density, the added powder must fill the void spaces without dilating the overall volume. For a random dense packing, the basic behavior is sketched in Figure 3. The packing volume, termed the specific volume (volume-to-mass ratio), is plotted as a function of the composition for a mixture of large and small spheres. There is a composition of maximum packing density that has a majority of large particles. The relative improvement in packing density depends on the particle size ratio of the large and small particles. Within a limited range, the greater the size ratio, the higher the maximum packing density. This is true up to a limiting size ratio of approximately 20:1, but requires at least a 20% difference in particle sizes [28,29].

Optimal Packing - The optimal packing density for a bimodal mixture of spheres corresponds to the minimum specific volume. At this optimal point the large particles are in point contact with one another and all of the interstitial voids are filled with small particles. A mathematical description of bimodal packing starts by designating the large particles with the subscript "L" and the small particles with the subscript "S". Calculation of the optimal composition in terms of the weight fraction of large particles X_L^* is an obvious goal. In general, the weight fraction of large particles at any composition X_L depends on the following equation:

$$X_L = \frac{W_L}{V_L + W_S} \quad (3)$$

with W indicating the weight. The weight of large particles is calculated from the theoretical density ρ_L , fractional packing density f_L , and container volume v as $W_L = f_L \rho_L v$.

For the condition of maximum packing density the desire is to add sufficient small particles to just fill the void space between the large particles, without forcing the large particles apart. The amount of void space equals $1 - f_L$, and the fractional packing density for the small particles times the volume and the theoretical density of the small particles gives its weight fraction as

$$W_S = (1 - f_L) f_S \rho_S v \quad (4)$$

Thus, the optimal packing X_L^* is given as follows:

$$X_L^* = \frac{f_L \rho_L}{f_L \rho_L + (1 - f_L) f_S \rho_S} \quad (5)$$

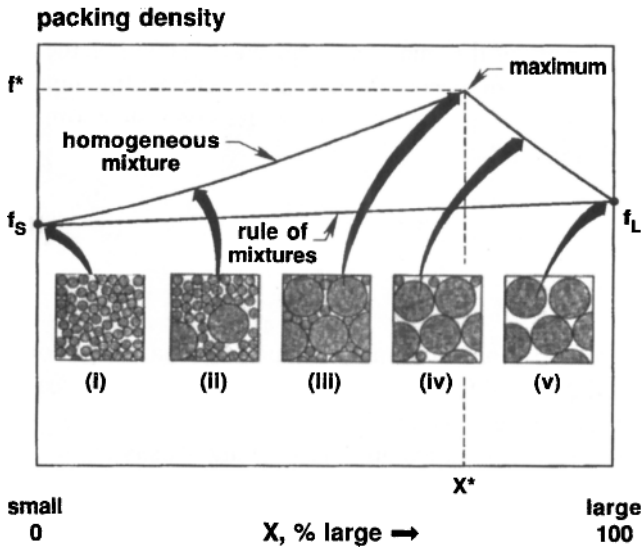


Figure 3. Packing with a bimodal size involves selection of smaller particles that fill the interstitial voids between the larger particles.

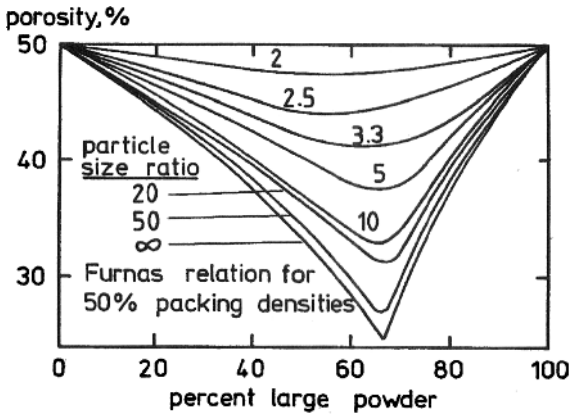


Figure 4. Porosity of various mixtures versus composition (percent large particles) and particle size ratio (large:small) to show how maximum packing density depends on both features.

In the case where the two particles composing the bimodal mixture are of the same composition, then the density of the small and large particles will be the same ($\rho_L = \rho_S$). A further simplification occurs for the case where the fractional packing densities for the two powders are the same. This case gives the optimal packing composition by the simple relation,

$$X_L^* = \frac{1}{2 - F_L} \quad (6)$$

Equations 5 and 6 give the compositions in terms of the proportional weight of large particles for the general case and for the specific case of equal theoretical densities and equal fractional packing densities.

Particle Size Ratio - Besides composition, the packing density is dependent on the particle size ratio up to a limit. The larger the particle size ratio, the higher the packing density at all compositions. For high packing densities, avoid porous and agglomerated particles. Consider two powders with a large difference in particle size, exhibiting random dense packing with the usual density of 63.7%. The corresponding weight fraction of large particles for maximum packing is 0.734, or 26.6 wt.% small particles.

For the more general cases, Figure 4 plots the porosity of mixed powders versus the percentage of the large powder. This plot shows the simultaneous effects of composition and particle size ratio (large divided by small) on the mixture density [30]. A minimum porosity occurs for each mixture at a composition rich in the large particles. The minimum porosity is larger and shifts toward the small particle axis as the particle size ratio decreases.

Figure 5 gives the relation between the inherent packing density of the large particles and the amount of small particles needed to attain maximum packing density as calculated by Furnas [29]. There is no gain in packing density if the particles have the same size, whereas the packing benefit is maximized by a large difference in particle sizes. Figure 6 shows the measurements by McGearry [24] for random dense packings. The fractional packing density increases as the particle size ratio increases up to a ratio of 15:1 or so. Note the change in behavior at the particle size ratio corresponding to a particle just filling the triangular pores between the large particles at roughly a 7:1 size ratio. The packing density is unchanged by particle size ratios larger than 20:1. In the size ratio range from 1:1 to 20:1 for D_L/D_S there is a major change in packing density. Figure 7 compares the prediction of Furnas [29] with that of Fedors and Landel [30]. The porosity of the mixture is expressed as a function of the inverse particle size ratio. Both models show that major packing benefits are associated with large

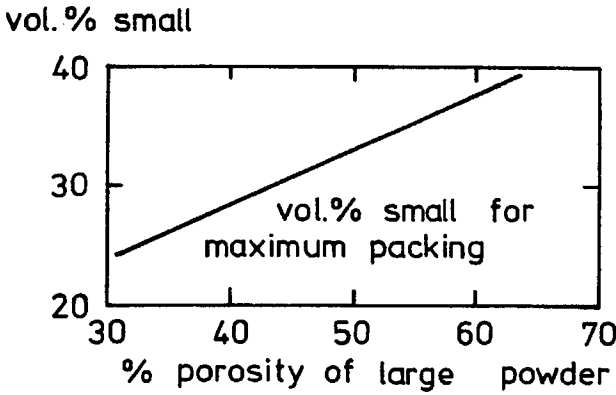


Figure 5. The amount of small powder in a bimodal mixture at the optimal packing condition as a function of the packing density of the large powder.

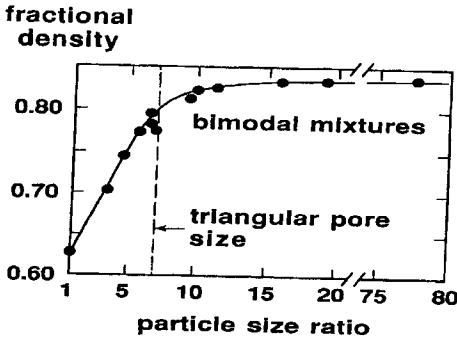


Figure 6. Experimental results from McGearry showing how the particle size ratio (large:small) impacts on the packing density for bimodal mixtures of spheres at the maximum packing density.

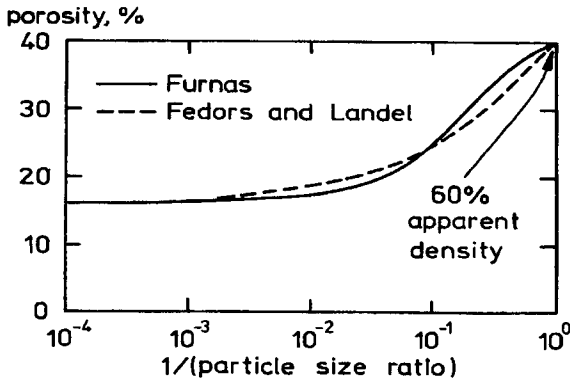


Figure 7. A comparison of the predicted bimodal powder packing density behavior for powders that pack to 60% density, showing the mixture porosity versus inverse particle size ratio for the models by Furnas and Fedors and Landel.

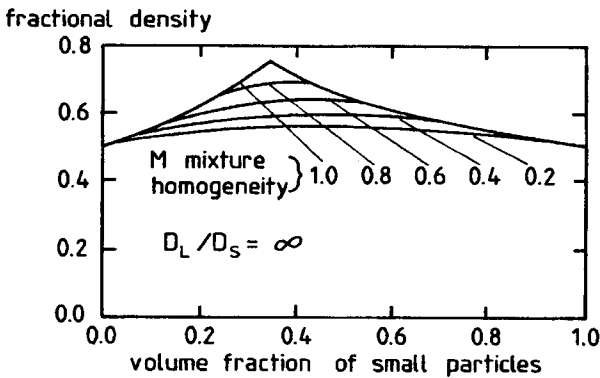


Figure 8. Homogeneity has impact on the fraction packing density in the same manner as the large:small particle size ratio. This plot shows density variation with composition for a large size ratio, but varying homogeneity.

differences in sphere sizes, but very large differences have no further benefit.

Mixture Homogeneity - Since the packing density varies with composition for mixtures of differing particle sizes, mixture homogeneity has a major effect on the packing density [23]. In an inhomogeneous packing, some regions will have more large particles than others. Consequently, the fractional density will vary from point-to-point in proportion to the local composition. Most models assume orderly positioning of the particles. In reality this is a difficult state to attain. Accordingly, the predicted density for a random bimodal mixture often overestimates that attainable in actual mixtures.

The packing density will increase with the homogeneity of the mixture. Figure 8 shows how composition and the degree of mixing will influence the packing density. This plots the fractional packing density versus composition for several levels of mixture homogeneity for an infinite particle size ratio. The density improves with the degree of mixing. The upper limit is based on perfect mixing, while the lower limit assumes a totally segregated structure. Randomly mixed systems will range between the unmixed and fully mixed limits, depending on the mixture homogeneity. The mixture homogeneity M is defined as follows:

$$M = 1 - \frac{\sigma}{\sigma_o} \quad (7)$$

where σ is the standard deviation in the composition between random samples taken from the mixture and σ_o is the standard deviation in composition for the unmixed system,

$$\sigma_o = \left(X_L (1 - X_L) \right)^{1/2} \quad (8)$$

Most random mixtures exhibit a homogeneity near 0.7. However, in well mixed ceramic powder systems an effective polymer can prevent segregation. Thus, slurry processing generally gives a higher homogeneity when compared to dry processing and binders contribute to a higher packing density.

A high packing density for the individual component particles is helpful in attaining a high packing density for the mixture. In the case of randomly packed monosized spheres with a density of 63.7%, a mixture of 73% large and 27% small will give a mixture packing density approaching 86%. The larger the particle size ratio and the more uniform the mixture homogeneity, then the closer the observed packing density will approach the model limits. All of the concepts addressed here for spheres carry over into mixtures of nonspherical particles, but

often the starting densities are lower because of inhibited packing.

MULTIPLE MODE DISTRIBUTIONS

The ideas developed for bimodal spherical packings have been extended to multiple mode systems. The first step is to consider trimodal mixtures, where there are three particle sizes. Subsequently, the trimodal systems form the basis for considering multiple mode mixtures (mixtures of several different monosized powders) and continuous particle size distributions. The continuous particle size distribution is of great interest since it is a practical approach to creating high packing density systems. As with bimodal packing, mixture homogeneity influences packing density for multiple mode or continuous distributions.

A few comments are in order about the practical aspects of multiple mode mixtures. It is often claimed that at least a 7:1 particle size ratio is needed for optimal packing. For a trimodal packing, this corresponds to a size ratio of 49:7:1. Assuming the smallest particles are 1 μm in size, then the largest particles will be 49 μm . Such a size is within a realistic working range. However, the classification of particles into sizes of 1, 7, and 49 μm is difficult. Obviously, as the size ratio or number of size classes becomes larger the practical problems increase. Consequently, continuous particle size distributions are more typical in practice.

The maximum packing density for bimodal mixtures of spheres is probably near 86%, whereas that of monosized spheres is 64%. This corresponds to a 34% improvement in packing. For a trimodal mixture, the maximum packing density is probably 95%. This is slightly more than a 10% improvement in packing over the bimodal situation. The addition of more components will return a decreasing benefit in packing, but the practical problems in preparing such mixtures may be insurmountable. Hence, a clear case can be made for bimodal mixtures in certain instances of ceramic processing, because of the large packing gain and relative ease of finding adequately different sizes. Mixtures formed from more components may not be fruitful.

The trimodal mixture of monosized spheres is very sensitive to the particle size ratio. For this discussion, the ternary sizes will be termed large, medium, and small. Depending on the ratio of sizes, a ternary mixture may have a higher packing density than the large-small binary. It is a key characteristic of all multiple mode powder mixtures that a large difference in particle sizes aids packing. Furnas [29] calculated, based on the particle size ratio, whether optimal packing would occur in the binary, ternary, or higher-order system; the results are shown in Figure 9. For a given particle size ratio and 60% inherent packing density, this plot indicates the number of components corresponding to optimal packing. For example, with a small particle size ratio such as 2, optimal packing

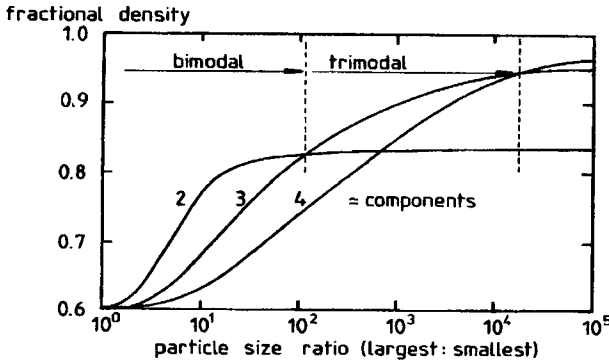


Figure 9. The effect of particle size ratio (large:small) on the packing density, showing how the selection of bimodal versus trimodal compositions depends on the available range of powder sizes.

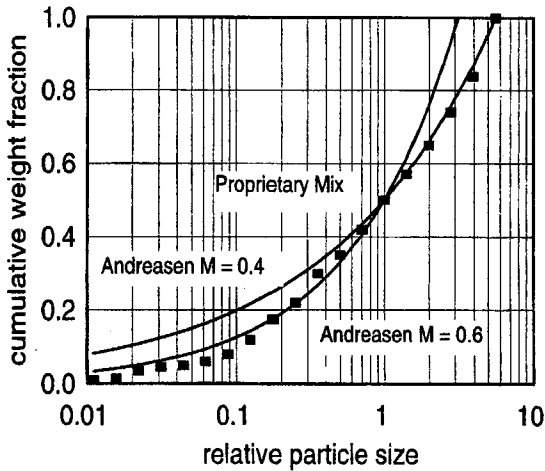


Figure 10. The Andreasen continuous particle size distribution with high packing densities has a skewed character with a high proportion of large particles and a long tail of small particles. Three distributions are included in the log size plot, showing a proprietary mixture for high solids loading as compared with the distributions identified by Andreasen.

occurs with two components. Alternatively, with larger particle size differences, like 1000:1, better packing would be attained with a ternary mixture.

It is noteworthy to examine the number of particles corresponding to optimal multiple mode packings. For a particle size ratio of 1:7:77, the volume percentages for each powder at optimal packing are 10, 23, and 67, respectively. The approximate number of particles corresponds to 69000, 490, and 1 for the small, medium, and large size classes. This means that a few large particles (but a high weight fraction) go a long way toward filling space. In the limiting case of an infinite particle size ratio, Lee [31] calculates a maximum packing density of 92.6% at a composition (by volume) of 8.7% small, 24.2% medium, and 67.1% large particles. For spheres with an inherent random packing density of 64%, the maximum density available with a trimodal mixture at an infinite particle size ratio is at 95% [32].

Further consideration of mixed particle sizes leads to four, five, and more components. As the number of components increases, the experimentation necessary to find an optimal packing composition becomes more difficult. One of the early treatments of multiple mode packing was performed by Horsfield [33]. For a mixture of 4 or 5 components, packing densities near 85% were demonstrated with modest size differences. At the extreme, a 6 component mixture with 96% density is possible. McGearry [24] experimentally produced a packing density of 95% in a random packing.

In multiple mode models, the structure takes its basic form from the largest particles, being sensitive to their size, shape and distribution [34]. The remaining void volume is then filled by the smaller particles. These in turn leave smaller pores that are filled by smaller particles. The effect of a small particle size ratio is a decrease in the maximum packing fraction. Using this concept, Furnas predicts maximum packing densities of 87, 95, 98, and 99% for 2, 3, 4, and 5 component systems.

CONTINUOUS PARTICLE SIZE DISTRIBUTIONS

From multiple mode packings it is obvious to extend the concepts to continuous distributions. The packing density of a multiple mode particle mixture increases as the number of components increases, as long as the particles are very different in size and an optimal composition is maintained. From this concept, a wide particle size distribution gives a higher packing density than with a narrow particle size distribution.

Sohn and Moreland [35] used Gaussian distributions to show the packing density increased with wider particle size distributions, independent of the mean particle size. However, there was a particle shape effect, with irregular particles giving a lower packing density.

For limited size widths, the packing density increases as the distribution becomes broader. With wide size distributions the packing density approaches a limiting value. For an infinitely wide particle size distribution, the projected packing density has been estimated to range between 82 and 96%. These values are comparable with the densities attainable with bimodal and trimodal mixtures with large particle size ratios. It is speculated that an upper density of 96% might be obtained with a very wide particle size distribution.

Furnas [29] showed a wide size distribution provided a high packing density and he describes a mixture process to secure a high density. His distribution was similar to the empirical findings of Fuller and Thompson [36]. Many subsequent measurements confirm these ideas [3]. More commonly, high packing densities are fit with a particle size distribution described by the Andraesen equation [37]:

$$W(D) = A_0 + A D^M \tag{9}$$

where W is the weight fraction of particles less than size D , and A_0 , A and M are empirical constants used to fit the particle size distribution. The maximum apparent density occurs for M values between 0.5 and 0.67, while M values between 0.33 and 0.5 give the highest tap density. Figure 10 plots the Andraesen distribution, showing the characteristic long tail of small particles and rapid rise in larger particles. For comparison, a proprietary high packing density mixture with low viscosity is included to show agreement with this simple model. A high proportion of small particles helps fill the voids between the nearly-continuous matrix of large particles.

Funk and Dinger [15] suggest a similar continuous particle size distribution function which traces directly to the Andraesen equation, but requires knowledge on the largest D_L and smallest D_s particle sizes,

$$W(D) = \frac{D^N - D_s^N}{D_L^N - D_s^N} \tag{10}$$

Again W represents the weight fraction of particles smaller than size D , and N is an adjustable constant to fit the distribution. Rearranging Equation 10 gives a form identical to Equation 9,

$$W(D) = A_1 + A_2 D^N \tag{11}$$

where the constants are defined by characteristics particle sizes such that $A_1 = 1/(D_L^N - D_S^N)$ and $A_2 = -D_S^N/(D_L^N - D_S^N)$. Further, by definition $W = 0.5$ at D_{50} (the median particle size), thus $D_{50}^N = (D_L^N + D_S^N)/2$, which defines N as a function of the three particle sizes. As demonstrated in Figure 11, this distribution function gives the same result as the Andreasen model.

Continuous particle size distributions can be mixed to improve the packing density if the mean sizes of the two distributions are very different. Lewis and Goldman [38] successfully argue that the mixture that gives optimal mixing corresponds to the widest particle size distribution. Thus, with continuous particle size distributions the key is to seek wide distributions to increase packing density and to form low viscosity suspensions.

RHEOLOGY LINKS

Most powder forming technology relies on particle lubrication from a fluid phase to assist in shaping. The fluid phase is divided into two partitions - that portion needed to fill all voids when the powder is at the maximum packing density (termed the immobile fluid) and the excess fluid that provides lubrication (termed the mobile fluid). These are saturated suspensions with all pore space filled with fluid. It is the extra fluid from dilation to a lower packing density than the maximum packing density that ensures lubricated particle flow. Schematically, this concept is sketched in Figure 12. It is the thickness of the lubricating layer between particles that determines suspension viscosity [39].

A viscous suspension as consists of discrete particles with all of the pores between the particles filled with fluid. It is the lubricating layer thickness that determines viscosity; hence, a linkage is needed between the layer thickness and the solid content in the suspension, known as the solids loading. As long as the particles are relatively large, typically not colloids, then at the critical solids loading the particles are in point contact, reflecting the same condition as the maximum packing density. If the solids loading is below the critical level, meaning that the powder is below the maximum packing density, then the excess fluid lubricates the particles.

Associated with this powder-fluid structure are concerns with strength and viscosity. Strength measures the stress needed to initiate flow and viscosity measures the stress needed to sustain flow. The higher the desired flow rate, typically the greater the stress. Particles have a natural tendency to adhere and agglomerate, leading to a low yield strength. Flow is initiated once the applied stress exceeds the yield strength, which increases with shear strain rate and solids loading. Typically this strength is low (in the range of 100 Pa or less) and can be ignored, but it is beneficial in holding shape after forming.

It is the excess fluid, termed the mobile fluid, that provides lubricity and